

# SAND–EPS GEOFOAM INTERFACE BEHAVIOR: A CONCEPTUAL FRAMEWORK AND EXPERIMENTAL RESULTS

V. C. Xenaki<sup>1</sup> and G. A. Athanasopoulos<sup>2</sup>

## ABSTRACT

A phenomenological conceptual framework for describing the EPS geofoam-sand interface behavior is proposed in this paper. Then the results of laboratory direct shear tests conducted at the EPS geofoam-sand interface are presented in the form of  $\tau$  versus  $\sigma_n$  failure envelopes. The observed interface behavior is explained using the conceptual framework which in terms of the degree of penetration of sand particles into the geofoam. The sands used in the tests were composed of well rounded to subangular particles with values of mean particle size ranging from 0.28mm to 2.17mm and void ratios ranging from 0.51 to 0.72. The EPS geofoam was of two different densities: 10kg/m<sup>3</sup> and 20kg/m<sup>3</sup>. The resulting failure envelopes have a non-linear form indicating a gradual transition from a ‘frictional’ type to ‘adhesional’ type of interaction for increasing values of interfacial normal stress. The predictions of the conceptual framework regarding the effect of important parameters are in agreement with the experimental results indicating that the interaction mechanism is mainly affected by the mean particle size and shape of sand as well as by the EPS geofoam density whereas the effect of sand void ratio is negligible. Values of interface friction angle and adhesion are proposed for the materials tested and for specific ranges of normal interfacial stresses that can be used in practical applications.

**KEYWORDS:** Expanded polystyrene, Geofoam, Sand, Direct shear test, Interface, Interface friction angle, Interface adhesion.

---

<sup>1</sup>Graduate Student, Dept. of Civil Engineering, University of Patras, Department of Civil Engineering, University of Patras, GR-26500 Patras, GREECE

<sup>2</sup>Professor, Dept. of Civil Engineering, University of Patras, Department of Civil Engineering, University of Patras, GR-26500 Patras, GREECE

## INTRODUCTION

In order to properly model and analyze composite ‘soil+EPS geofoam’ system under static and dynamic loading and proceed to the engineering design of the relevant technical works it is necessary to have information on the mechanical behavior of EPS geofoam and on the interaction mechanism at the interface between soil and EPS geofoam. Such information has started appearing in the technical literature (Athanasopoulos et al. 1999) but much remains to be learned, especially on the subject of interfacial behavior. The majority of geofoam applications, according to Horvath (1994, 1995) and Negusse (1998), involve the use of expanded polystyrene (EPS) which is usually utilized in the form of molded blocks.

According to Horvath (1995, 1997) EPS geofoam blocks are used today in a wide range of geotechnical applications including the following: 1) Thermal Insulation, 2) Lightweight Fill, 3) Compressible Inclusion and 4) Vibration Damping. A potential application of EPS geofoam which is presently under investigation is its use as a seismic buffer behind earth retaining walls (Inglis et al. 1996, Bathurst and Alfaro 1996). In a recent publication Pelekis et al. (2000) presented the results of a finite element study on the subject indicating a significant decrease of seismic earth pressures acting on cantilever-type retaining walls protected by a layer of EPS geofoam placed at the wall-backfill interface.

The mechanical properties of EPS geofoam, whose knowledge is required when designing geotechnical applications based on the previously mentioned functions, have been the subject of many investigations in the past few years. As far as the mechanical properties of EPS geofoam under static loading conditions are concerned, a considerable amount of research work is available and has already been reported in the literature during the last years (Horvath 1995, Preber et al. 1994, Athanasopoulos et al. 1999). Less experimental data are available, however, concerning the mechanical properties under dynamic/cyclic/seismic loading conditions (Duškov 1997, Athanasopoulos et al. 1999). Also, regarding the interaction mechanism at the geofoam-soil interface no data seem to be, at present, available in the technical literature. A knowledge of this interfacial behavior is essential, however, when analyzing the behavior of composite systems (soil+EPS geofoam) under cyclic/dynamic/seismic loading and particularly for the investigation of the potential use of EPS geofoam for the seismic isolation of earth retaining structures.

In the present study, a conceptual framework for describing the EPS geofoam-sand interface behavior is first proposed. Then the results of an experimental investigation of the interaction mechanism at the EPS geofoam-sand interface by laboratory direct shear testing are presented and compared to the predictions of the conceptual framework. The dependence of the interfacial behavior on the EPS geofoam density,  $\rho$ , void ratio of sand,  $e$ , mean particle size of sand,  $D_{50}$ , and particle shape is examined. The interface behavior is described by  $\tau$  versus  $\sigma_n$  envelopes (where  $\tau$  and  $\sigma_n$  are the interfacial shear and normal stresses) from which apparent values of interface friction angle,  $\delta$ , and adhesion,  $c_a$ , can be estimated.

## REVIEW OF PREVIOUS WORK

Most of the previous research work on EPS geofoam has focused on the mechanical properties of the material in both the static and dynamic loading ranges. Several researchers have reported experimental data concerning the mechanical behavior of EPS geofoam under static loading conditions (Horvath 1995, Preber et al. 1994, Athanasopoulos et al. 1999). The mechanical properties of EPS geofoam under dynamic/cyclic loading have been the subject of a few investigations in recent years. Athanasopoulos et al. (1999) have found that EPS geofoam behaves linearly, in terms of dynamic stress-strain behavior for cyclic strain amplitudes up to 0.1%. Beyond this strain limit the EPS geofoam exhibits non linear behavior which becomes more pronounced for strain amplitudes greater than 1%.

It has been also found by Athanasopoulos et al. (1999) that 1) the dynamic modulus of EPS geofoam increases with the density of the material, whereas the damping ratio is practically unaffected by this important physical index property of the material, 2) the value of Poisson's ratio,  $\nu$ , is close to zero and may even become negative

and 3) the cyclic strain amplitude has a pronounced effect on the elastic moduli ( $E$ ,  $G$ ) and the damping ratio,  $D$ , of EPS geofoam. Equations for  $G/G_0$  versus  $\gamma_c$  and  $D$  versus  $\gamma_c$  curves ( $G_0$ =shear modulus for low amplitude vibrations) for EPS geofoam have been developed based on the results of resonant column and cyclic triaxial tests. These curves describing the non-linear behavior of EPS geofoam have been used for seismic response analyses of earth retaining walls seismically isolated with EPS geofoam layers by Pelekis et al. (2000).

To the best of authors' knowledge no data are available in the literature for the interaction mechanism at the EPS geofoam-sand interface. A few experimental results concerning the shear strength of granular material- "smooth" high density polyethylene (HDPE) geomembrane interfaces are available. According to Zettler et al. (2000) the interfacial shear strength results predominantly from plowing and sliding of the particles at the interface. The relative contribution of particle sliding and plowing for a given "smooth" geomembrane surface is a function of the relative material hardness, the particle size and angularity, the normal stress and the material density. Consequently, the strength of the interface is directly related to the ability of soil particles at the interface to plow into the geomembrane surface. Sliding along the interface requires minimal work by the particle. However, significant effort is required for the particle to plow into the surface of the geomembrane resulting in increased interfacial strength and increased surface roughness. As shown in Figure 1, at low normal stresses the soil particles slide along the geomembrane surface, whereas plowing does not occur. Therefore, the surface roughness is not significantly affected. However, beyond a transition point of approximately 100kPa the soil particles plow into the geomembrane surface and the interfacial shear strength is increased due to the significant increase in surface roughness.

## CONCEPTUAL FRAMEWORK FOR THE INTERFACIAL BEHAVIOR

The interaction mechanism at the EPS geofoam-sand interface can be described by a conceptual framework that is shown graphically in Figure 2. The main concepts used in the framework are 1) the number of geofoam-sand contact points per unit interfacial area and 2) the degree of penetration of each sand particle into the geofoam material.

The number of contact points obviously depends on the mean size of sand particles and the value of void ratio and it should be expected that the shearing resistance at the interface increases with the number of contact points. Simple calculations, based on the assumption of idealized spherical particles of equal diameter, indicate that for a particle size decrease from 2.17mm to 0.28mm (87% decrease), the number of contacts per unit area increases by 5900% !

The void ratio,  $e$ , of the sand would also be expected to affect the number of contact points. A calculation of the number of contacts per unit area for two different arrangements of the sand particles indicates that a 25% decrease of void ratio value results in a 15% increase of number of contacts per unit area. Based on the above calculations and by taking into consideration the usual ranges of void ratios (0.4 to 0.9) and particle sizes (0.075mm to 4.75mm) of sandy soils it may be concluded that the effect of void ratio on the EPS geofoam-sand interface mechanism is insignificant compared to the effect of particle size.

As mentioned above the interaction mechanism would also be expected to be affected by the degree of penetration of sand particles into geofoam. This penetration is expected to increase with the interfacial normal stress and the angularity of the particle (Figure 2). When the normal interfacial stress is low (Phase A) the degree of penetration is negligible. Rolling (or possibly sliding) of sand particles along the interface occurs and the shearing surface is shifted above the interface and entirely located in the sand. Consequently, the interaction mechanism is expected to be purely frictional. In Phase B (intermediate normal interfacial stress) a number of sand particles has penetrated into geofoam forcing parts of the shearing surface to move into geofoam. The interfacial behavior can be described as frictional-adhesional whereupon a part of the shearing resistance is derived by the frictional resistance of sand whereas the remaining part is derived by the shearing resistance of geofoam. Finally, when the interfacial normal stress is high (Phase C) most sand particles have penetrated into the geofoam surface. Consequently, the shearing surface is located entirely in the EPS geofoam and the interaction mechanism is purely adhesional.

## MATERIALS TESTED

The experimental investigation reported in the current study was conducted in the Laboratory of Geotechnical Engineering, Department of Civil Engineering, University of Patras, Greece by using a direct shear apparatus with a square shear box. Three types of sand were used in the tests as well as EPS geofoam samples of two different densities.

To establish the main characteristics of the interaction mechanism at the EPS geofoam-sand interface a number of tests were conducted by using Ottawa sand 20-30 with well rounded particles. These tests were followed by tests conducted on a natural beach sand. To investigate the effect of the mean particle size of sand,  $D_{50}$ , on the interfacial behavior, two fractions of the beach sand were selected for the present study. Beach sand-1 (8-10) was the fraction of sand passing the No 8 standard sieve and retained by the No 10 sieve, thus having mean particle size,  $D_{50}$ , equal to 2.17mm. Beach sand-2 was similarly obtained by using standard sieves No 40 and No 100. The mean particle size,  $D_{50}$ , of this sand is equal to 0.28mm. The shape of the beach sand particles is subrounded to subangular in contrast to the well rounded Ottawa sand particles.

The EPS geofoam samples used in the present study were supplied by an EPS molder in the form of prismatic blocks. The test specimens (right parallelepipeds in shape) were cut and trimmed from the EPS blocks to the required dimensions. In order to investigate the effect of EPS geofoam density on the interaction mechanism at the EPS geofoam-sand interface, specimens of EPS geofoam with mean densities,  $\rho$ , equal to  $10\text{kg/m}^3$  and  $20\text{kg/m}^3$  were used. These specimens are denoted in the present study as EPS10 and EPS20, respectively. EPS10 and EPS20 were used in the current study because these relatively light geofoam materials seem to be better suited for compressive inclusion and seismic buffer applications.

## EXPERIMENTAL PROGRAM

The interaction mechanism at the EPS geofoam-sand interface was investigated in the present study by conducting interface direct shear tests in a conventional laboratory direct shear apparatus with 100mm x 100mm shear box. The interfacial direct shear tests were conducted by filling the lower half of the shear box with sand and placing on its surface an EPS geofoam specimen cut to appropriate dimensions (smaller than the shear box dimensions) to fit in the upper half of the shear box. Direct shear tests with the shear box filled completely with sand were also conducted to evaluate the angle of internal friction,  $\phi$ , of all sands used in this investigation. The rate of shearing was 0.4mm/min in all tests. Each test was normally terminated when the shear displacement,  $\Delta h$ , reached the value of 10mm.

The experimental program was designed in such a way as to allow the investigation of the effect of important parameters on the interfacial interaction mechanism, namely the EPS geofoam density, the normal interfacial stress, the size and shape of sand particles and the void ratio of sand.

The experimental program included a series of 52 tests conducted on dry Ottawa sand 20-30 in contact with EPS10 and EPS20 geofoam. In these tests the void ratio of sand was 0.51 and the interfacial normal stress ranged from 2.1kPa to 78.5kPa. The angle of internal friction of Ottawa sand 20-30 was found to be  $\phi=36^\circ$ . The aim of this series of tests was to allow the establishment of the general characteristics of the interfacial behavior and the development of the conceptual framework explaining the observed behavior.

The experimental program also encompassed 114 tests on the two fractions of the beach sand. Beach sand-1 was tested for two values of void ratio (dense and loose conditions): 0.51 and 0.72 whereas Beach sand-2 was tested for void ratio values of 0.60 and 0.72. The tests of these series were conducted for both EPS geofoam densities: EPS10 and EPS20. The values of interfacial normal stress in these tests ranged from 2.0kPa to 70kPa. Table 1 summarizes the characteristics of tested sands, including the values of their friction angles.

## TEST RESULTS AND DISCUSSION

The results of direct shear tests in the form of  $\tau$ - $\sigma_n$  failure envelopes are used in this section to establish the basic characteristics of the interaction mechanism and draw conclusions on parameter effects.

### Comparison to the Predictions of Conceptual Framework

The results of tests on Ottawa sand 20-30 are summarized in Figure 3. The failure envelopes of EPS10-sand and EPS20-sand interfaces are compared in this diagram to the failure envelope of Ottawa sand 20-30. It should be noted that the curves shown in Figure 3 are best fit curves to the test data, characterized by very high values of correlation coefficients. This type of presentation was chosen to facilitate the comparison of the curves.

According to the diagram of Figure 3 the interaction behavior at the EPS geofoam-sand interface can be represented by a non-linear failure envelope. The test results indicate that for low values of normal interfacial stress the apparent friction angle,  $\delta$ , between EPS geofoam and sand is approximately equal to the friction angle of sand. Thus, for  $\sigma_n$  values up to 10kPa or 2.5kPa for the EPS10 or EPS20 geofoams, respectively, the interaction behavior may be characterized as ‘‘frictional’’ in nature. For higher values of normal interfacial stress the behavior becomes ‘‘frictional-adhesional’’ in nature, indicating continuously decreasing values of interface friction angle,  $\delta$ , and increasing values of apparent interface adhesion,  $c_a$ . Finally, above a certain critical value of normal interfacial stress the interfacial behavior becomes purely ‘‘adhesional’’. For the case of EPS10 this critical value of normal interfacial stress is approximately equal to 35kPa whereas for the case of EPS20 the critical value seems to be greater than 78.5kPa (the maximum value of normal stress used in the tests).

The observed behavior at the EPS geofoam-Ottawa sand interface can be explained in terms of the conceptual framework described above. Based on the framework depicted in Figure 2, the three phases of interaction observed in Figure 3 for the Ottawa sand-EPS geofoam system can be interpreted in terms of different degrees of penetration. In Phase A (Figure 2a) the normal interfacial stress is very low resulting in a negligible degree of penetration. Consequently the shearing surface is located entirely above the interface and the interaction mechanism is expected to be purely frictional. In Phase B a number of sand particles has penetrated into geofoam forcing parts of the shearing surface to move into geofoam. This results in a general type of interface behavior (frictional-adhesional) in which a part of the shearing resistance is derived by the frictional resistance of sand whereas the remaining part is derived by the shearing resistance of geofoam. Finally, in Phase C, all (or most) sand particles have penetrated into the geofoam surface and the shearing surface is located entirely in the EPS geofoam. The interaction mechanism is purely ‘‘adhesional’’ in this case and is characterized by an adhesion,  $c_{a \max}$ , since the interface resistance is derived entirely by the shear resistance offered by the geofoam. The value of the interface adhesion,  $c_{a \max}$ , is expected to be equal to the shearing resistance of EPS geofoam at a strain value corresponding to the shear displacement developed in the shear zone. It would also be expected that the value of  $c_{a \max}$  is increasing with the density of EPS geofoam (a fact that is actually observed in Figure 3).

### Parameter Effects on the Interaction Mechanism

The results of direct shear tests on the EPS geofoam-beach sand interface were utilized in order to study the effects of interfacial normal stress, geofoam density and particle size and void ratio of sand.

The diagram of Figure 4 depicts the failure envelope of Beach sand-1 and the interface failure envelopes for EPS10 and EPS20, for a value of void ratio equal to 0.51 (dense conditions). It can be easily observed that the interface behavior for this sand bears great similarity to the behavior depicted in Figure 3 for Ottawa sand 20-30. It is, also, worth noting that the value of normal interfacial stress at which the EPS10 and EPS20 curves are

intersecting is 25kPa for Beach sand-1 and 40kPa for Ottawa sand 20-30. This difference is readily explained by the conceptual framework presented above in terms of the different particle shapes of the two sands: according to Table 1, Ottawa sand 20-30 is composed of well rounded particles whereas Beach sand-1 has subrounded particles. Obviously, greater values of normal stress are required to achieve a degree of particle penetration of the well rounded Ottawa sand 20-30 into geofoam material equal to that corresponding to the subrounded Beach sand-1.

A similar trend is observed in the diagram of Figure 5 which depicts the effect of EPS geofoam density for the case of Beach sand-2. It is noted that the failure envelope of this finer grained sand indicates the existence of a small cohesion intercept. The value of interfacial normal stress at which the two geofoam curves intersect is even smaller in this case: 15kPa. Again this may be explained by the fact that the shape of Beach sand-2 particles is more angular than that of Beach sand-1.

Regarding the effect of EPS geofoam density on the shape of interface failure envelope, based on the results shown in Figures 3, 4 and 5, it may be concluded that for low normal interfacial stress (below 35kPa to 15kPa) the EPS10 material develops higher shearing resistance than the EPS20 material. For higher values of normal stress, however, the interface shearing resistance increases with the EPS geofoam density. The proposed conceptual framework again offers the following explanation for this behavior. For a given value of normal interfacial stress a sand particle penetrates easier into the soft EPS10 material. This results in a higher shearing resistance contribution from this geofoam material compared to the stiffer EPS20 material into which a lower degree of penetration is occurring.

The effect of void ratio of sand on the interfacial behavior is demonstrated in the diagram of Figure 6 for EPS20 geofoam and Beach sand-2. It may be seen in this diagram that a variation of void ratio from 0.60 to 0.72 for Beach sand-2 did not produce any appreciable change in the interfacial behavior. This is in agreement with the predictions of the conceptual framework proposed in a previous section.

Finally, the effect of sand particle size on the interface behavior is clearly demonstrated in the diagrams of Figures 7 and 8 for dense conditions and both EPS10 and EPS20 geofoams. In both diagrams the failure envelope for finer grained sand ( $D_{50}=0.28\text{mm}$ ) is located above the envelope for the coarser sand ( $D_{50}=2.17\text{mm}$ ) as predicted by the conceptual framework. It may, therefore, be concluded that for a 7.5 times decrease of  $D_{50}$  of the sand (from 2.17mm to 0.28mm) the interface shearing resistance may be increased by 20% to 50%. It should be noted, however, that according to the diagram of Figure 7, the effect of  $D_{50}$  on the interface shear resistance diminishes with increasing values of normal interfacial stress.

## **Practical Implications**

The results of all direct shear tests conducted in this investigation at the interface of Beach sand-EPS10 are summarized in Figure 9, whereas the corresponding results for EPS20 are shown in Figure 10. In each of these two figures it is possible to draw a single average curve to describe the effect of normal stress on the interfacial shear resistance for all values of  $e$ ,  $D_{50}$  and particle shapes used in the tests. Although the scatter of data points around the average curve of Figure 10 cannot be neglected, nevertheless, this average curve may be useful when evaluating the interface parameters in practical applications.

Both curves are non-linear and may be approximated by a number of linear segments: The first linear segment corresponds to Phase A of the interaction mechanism, in which the interaction is predominantly frictional. Table 2 gives the values of apparent interface friction angle that can be used in applications involving the use of EPS10 and EPS20 as well as the corresponding normal stresses. The second linear segment, corresponds to Phase B of the interaction mechanism, in which the interaction involves both frictional and adhesional components. Apparent values of interface friction angle and adhesion are also included in Table 2 for both EPS geofoam densities. Finally, the third linear segment-which is not present in the case of EPS20-corresponds to Phase C of the interaction mechanism, in which the interaction has a purely adhesional component. An apparent value of

interface adhesion and the corresponding limiting values of normal interfacial stress, are given in Table 2 for the case of EPS10. For EPS20 the development of Phase C interaction mechanism would require values of normal interfacial stress higher than those applied in the current study.

The apparent values of  $\delta$  and  $c_a$  given in Table 2 can be used in analyses of applications involving the use of low density EPS geofoam ( $10\text{kg/m}^3$  or  $20\text{kg/m}^3$ ) in association with the corresponding limiting values of normal interfacial stress. For the case of sands with well rounded particles, values of  $\delta$  and  $c_a$  can be estimated from the test results of Ottawa sand 20-30, shown in Figure 3. In the aforementioned applications (e.g. compressible inclusion or seismic buffers in earth retaining structures) it is necessary to analyze the behavior of the composite system (soil+geofoam) by taking appropriately into consideration the interface behavior.

## SUMMARY

Based on the experimental results of the current study the following conclusions can be drawn:

1. The failure envelope ( $\tau$  versus  $\sigma_n$ ) at an EPS geofoam-sand interface is a non-linear curve with an initial portion tangential to the linear failure envelope of sand, and may be approximated by a piecewise linear curve. The initial linear segment of this curve, which develops for low values of normal interfacial stress, defines a frictional behavior, with an apparent interface friction angle,  $\delta$ , approximately equal to the friction angle of the sand. For higher values of normal interfacial stress the interaction behavior becomes progressively adhesional in nature. The value of angle  $\delta$  continuously decreases whereas an apparent adhesion is developed which gradually increases until it becomes equal to the shear resistance of EPS geofoam. This shear resistance corresponds to the shear strains developed in the shear zone as a result of the induced shear displacement.
2. A conceptual framework, phenomenological in nature, is proposed for the interpretation of the observed behavior at the EPS geofoam-sand interface. The degree of penetration of sand particles into the geofoam material, which is the fundamental concept of this framework, depends on the normal interfacial stress, the geofoam density, the size and shape of sand particles and the void ratio of sand.
3. The experimental results are in agreement with the predictions of the proposed framework regarding the parameter effects on the interaction mechanism:
  - The EPS geofoam density affects significantly the shape and position of the interfacial failure envelope. For EPS10 the interaction involves all three phases, whereas for EPS20 the phase of purely adhesional interaction is not developed for the practical range of normal interfacial stresses.
  - The mean particle size of sand,  $D_{50}$ , affects significantly the shearing resistance at the interface for the range of normal interfacial stresses used in the tests. A 20% to 50% increase of shearing resistance was observed in the current study by decreasing the  $D_{50}$  value from 2.17mm to 0.28mm.
  - The void ratio value of sand was not found to appreciably affect the interfacial shear resistance for the range of values (0.51 to 0.72) used in the tests.
  - The shape of sand particles affects appreciably the interfacial shear resistance. For the same value of normal interfacial stress, the shearing resistance increases with the degree of angularity of sand particles.
  - Based on the test results of the present study (void ratios ranging from 0.51 to 0.72,  $D_{50}$  values ranging from 0.28mm to 2.17mm and well rounded to subangular sand particles) values of interfacial friction and adhesion are proposed for specific ranges of normal interfacial stress and for EPS10 and EPS20 geofoams. These values may be used directly in practical applications involving similar sands and stress conditions with the ones used in the tests.

## ACKNOWLEDGEMENTS

The authors wish to express their thanks to the EPS molding factory of Patras, PATRAIKA MONOTIKA, for providing the prismatic blocks from which the EPS geofam test specimens were prepared. Thanks are also expressed to the civil engineering students of the University of Patras, Barbara Davoni and Sophia Plavou, for their careful experimental work in the direct shear tests on Ottawa sand 20-30.

## REFERENCES

- ASTM D 3080, *Standard Test Method for Direct Shear Test of Soils Under Consolidated Drained Conditions*, American Society for Testing and Materials, West Conshohocken, Pennsylvania, USA.
- Athanasopoulos, G. A., Pelekis, P. C. and Xenaki, V. C., (1999), "Dynamic Properties of EPS Geofam: An experimental Investigation", *Geosynthetics International*, Vol. 6, No. 3, pp. 171-194.
- Bathurst, R. J. and Alfaro, M.C. (1996), "Review of Seismic Design, Analysis and Performance of Geosynthetic Reinforced Walls, Slopes and Embankments", *Proceedings of the International Symposium on Earth Reinforcement*. Fukuoka, Kyushu, Japan, Nov. 1996, Ochiai H., Yasufuku N. and Omine K. Editors Balkema, 1997, Vol.2, pp. 887-915.
- Duřkov, M. 1997, "Materials Research on EPS-20 and EPS-15 Under Representative Conditions in Pavement Structures", *Geotextiles and Geomembranes*, Vol. 15, Nos. 1-3, pp. 147-181.
- Horvath, J. S., (1991), "The Case for an Additional Function", *IGS News*, International Geosynthetics Society, Vol. 7, No. 3, November 1991, pp. 17-18.
- Horvath, J. S., (1992), "New Developments in Geosynthetics ; 'Lite' Products Come of Age", *Standardization News*, ASTM, Vol.20, No.9, Sept.1992, pp. 50-53.
- Horvath, J. S., (1994), "Expanded Polystyrene (EPS) Geofam : An Introduction to Material Behavior", *Geotextiles and Geomembranes*, Vol.13, No. 4, pp. 263-280.
- Horvath, J. S., (1995), "*Geofoam Geosynthetic*", Horvath Engineering, P.C. Scarsdale, N.Y. U.S.A 217 p.
- Horvath J. S., (1997), "The Compressible Inclusion Function of EPS Geofam", *Geotextiles and Geomembranes*, Vol. 15, Nos. 1-3, pp. 77-119.
- Inglis, D., Macleod, G., Naesgaard, E. and Zergoun, M., (1996), "Basement Wall with Seismic Earth Pressure and Novel Expanded Polystyrene Foam Buffer Layer", *Proceedings of 10<sup>th</sup> Annual Symposium of the Vancouver Geotechnical Society*, Vancouver, B.C., 18p.
- Negusse, D., (1998), "Putting Polystyrene to Work", *Civil Engineering*, ASCE, March 1998, pp. 65-67.
- Pelekis, P. C., Xenaki, V. C. and Athanasopoulos, G. A., (2000), "Use of EPS Geofam for Seismic Isolation of Earth Retaining Structures: Results of a Finite Element Study", *Proceedings of Second European Geosynthetics Conference*, Bologna, Italy, October 2000, Vol. 2, pp. 843-846.
- Preber, T., Bang, S., Chung, Y. and Cho, Y., (1994), "Behavior of Expanded Polystyrene Blocks", *Transportation Research Record 1462*, pp. 36-46.
- Zettler, T. E., Frost, J. D. and DeJong, J. T., (2000), "Shear-Induced Changes in Smooth HDPE Geomembrane Surface Topography", *Geosynthetics International*, Vol. 7, No. 3, pp. 243-267.



Table 1 Characteristics of sands used in the tests

Sand type	Sand fraction (Sieve No.)	D <sub>50</sub> (mm)	Particle shape	Void ratio e (dimensionless)	Friction angle (°)
Ottawa sand	20-30	0.72	well-rounded	0.51	36
Beach sand-1	8-10	2.17	subrounded	0.51	41
				0.72	31
Beach sand-2	40-100	0.28	subangular	0.60	50
				0.72	40

Table 2 Proposed values of friction angle and adhesion at the EPS geofoam-sand interface for two EPS densities and specific ranges of normal interfacial stress

	EPS10			EPS20		
	$\sigma_n$ (kPa)	$\delta$ (°)	$c_a$ (kPa)	$\sigma_n$ (kPa)	$\delta$ (°)	$c_a$ (kPa)
Phase A	0 to 15	34	0	0 to 35	32	0
Phase B	15 to 30	19	5.5	> 35	15	13
Phase C	> 30	0	16.5			

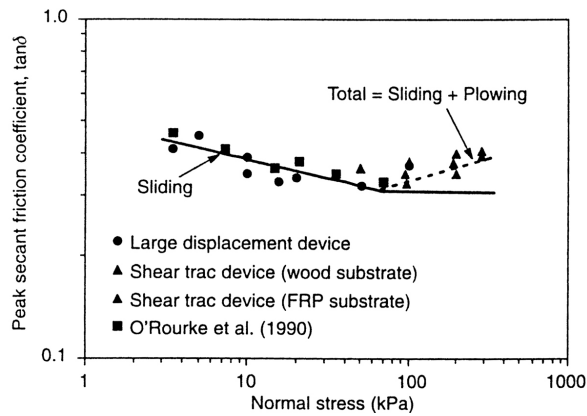


Figure 1 Smooth HDPE geomembrane-Ottawa 20/30 sand interface shear mechanisms (Zettler et al., 2000)

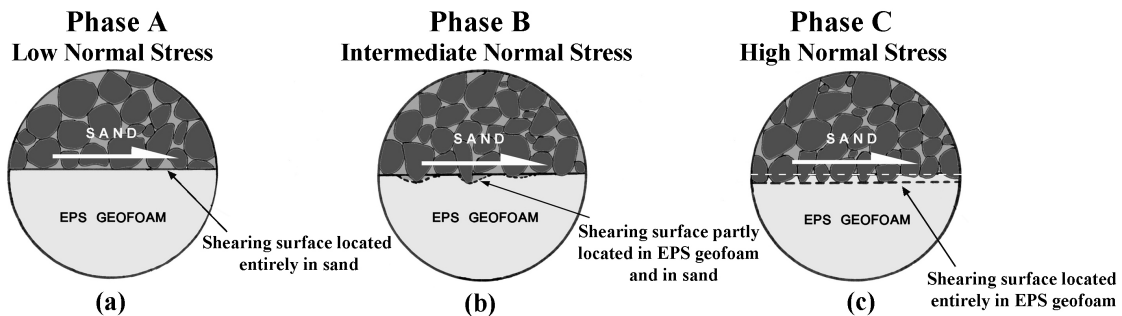


Figure 2 Conceptual framework the three interaction phases at the EPS geofoam-sand interface

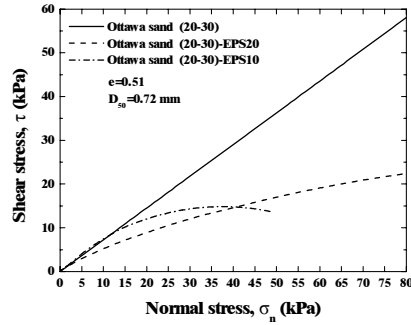


Figure 3 Effect of EPS density on the interaction behavior at EPS geofoam-Ottawa sand 20-30 interface

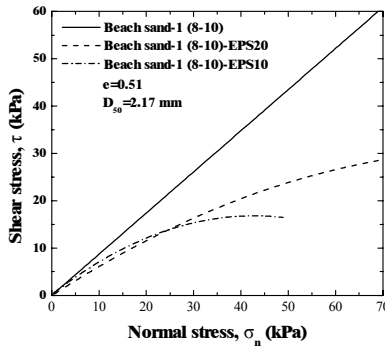


Figure 4 Effect of EPS density on the interaction behavior at the EPS geofoam-Beach sand-1 interface

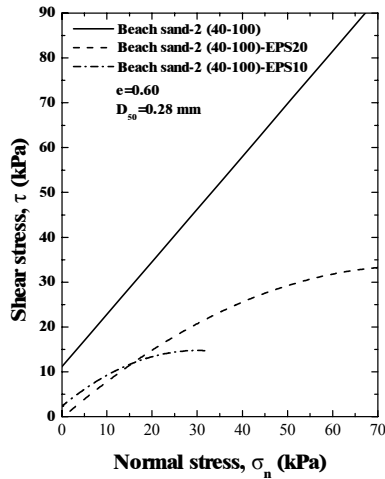


Figure 5 Effect of EPS density on the interaction behavior at the EPS geofoam-Beach sand-2 interface

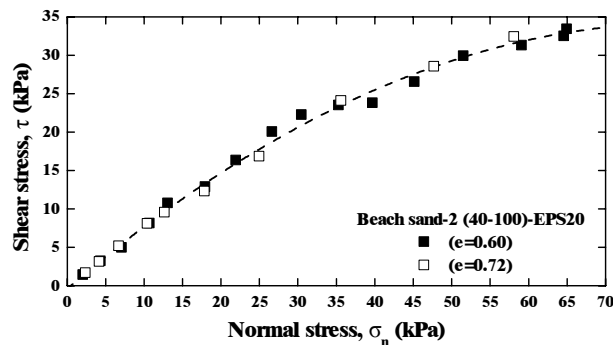


Figure 6 Effect of void ratio value on the interaction behavior at the EPS20-Beach sand-2 interface

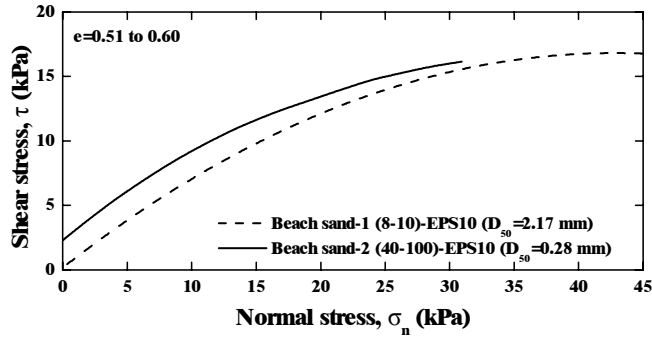


Figure 7 Effect of mean particle size on the interaction behavior of EPS10-Beach sand (dense conditions)

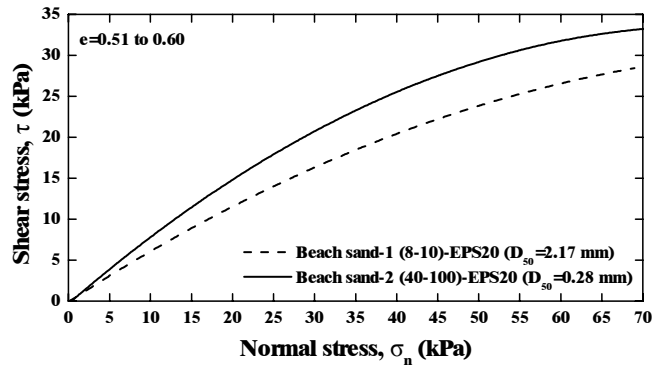


Figure 8 Effect of mean particle size on the interaction behavior of EPS20-Beach sand (dense conditions)

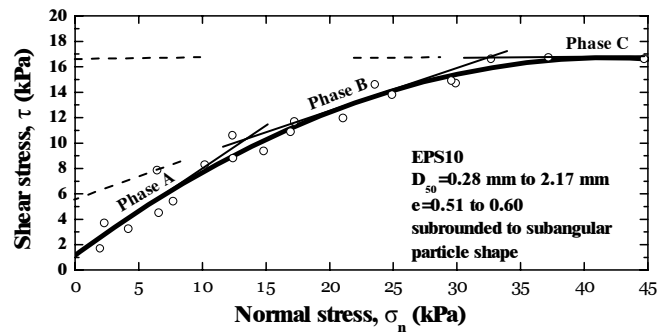


Figure 9 Proposed piecewise linear failure envelope at the EPS10-Beach sand interface, on the basis of experimental data

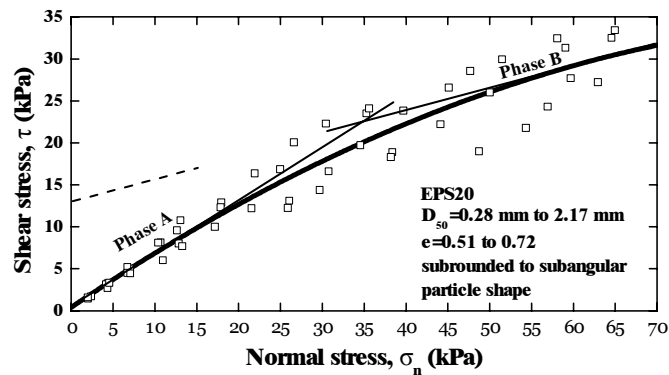


Figure 10 Proposed piecewise linear failure envelope at the EPS20-Beach sand interface, on the basis of experimental data